Dense packings of hard circular arcs

Juan Pedro Ramírez González
Departamento de Física Teórica de la Materia Condensada, Universidad Autónoma de Madrid, Ciudad Universitaria de Cantoblanco, E–28049 Madrid, Spain

Giorgio Cinacchi
Departamento de Física Teórica de la Materia Condensada, Instituto de Física de la Materia Condensada (IFIMAC), Instituto de Ciencias de Materiales "Nicolás Cabrera", Universidad Autónoma de Madrid, Ciudad Universitaria de Cantoblanco, E–28049 Madrid, Spain

(Received 15 July 2020; accepted 9 September 2020; published 12 October 2020)

This work investigates dense packings of congruent hard infinitesimally thin circular arcs in the two-dimensional Euclidean space. It focuses on those denotable as major whose subtended angle $\theta \in (\pi, 2\pi]$. Differently than those denotable as minor whose subtended angle $\theta \in [0, \pi]$, it is impossible for two hard infinitesimally thin circular arcs with $\theta \in (\pi, 2\pi]$ to arbitrarily closely approach once they are arranged in a configuration, e.g., on top of one another, replicable ad infinitum without introducing any overlap. This makes these hard concave particles, in spite of being infinitesimally thin, most densely pack with a finite number density. This raises the question as to what are these densest packings and what is the number density that they achieve. Supported by Monte Carlo numerical simulations, this work shows that one can analytically construct compact closed circular groups of hard major circular arcs in which a specific, θ-dependent, number of them (counter) clockwise intertwine. These compact closed circular groups then arrange on a triangular lattice. These analytically constructed densest-known packings are compared to corresponding results of Monte Carlo numerical simulations to assess whether they can spontaneously turn up.

DOI: 10.1103/PhysRevE.102.042903

I. INTRODUCTION

Systems of hard (i.e., noninteracting except for nonintersecting) particles are elementary model systems with which to investigate (condensed) states of matter [1,2]. Out of the many aspects of this investigation [3–8], one is the determination of those packings (i.e., single configurations) that exhibit the maximal density [4,8].

In the two-dimensional Euclidean space ($\mathbb{R}^2$), it has long been mathematically proven that hard circles, the simplest hard particles, most densely pack in a triangular lattice [9]. Equally mathematically proven has been that hard convex particles, if centrosymmetric, most densely pack in a lattice [10] while, if noncentrosymmetric, pack in a double lattice that covers, as a minimum, a fraction of $\mathbb{R}^2$ equal to $\frac{\sqrt{3}}{2}$ [11]. For hard concave particles, the sole conjecturing what may be the densest packings may not be immediate, leaving aside devising a convincing mathematical proof that these packings are such indeed. In this context, numerical methods, that originated in physics, such as the Monte Carlo and molecular dynamics methods [12–16], become increasingly useful. In two recent works, event-driven molecular dynamics was used to determine the densest-known packings of hard convex and concave superdiscs [17] while a method of the Monte Carlo type [18] was used to determine the densest-known packings of an ample variety of hard convex and concave particles [19].

Out of the many generalizations of a circle, one views it as a special circular arc. It is then natural to consider, as hard, generally noncircular, particles, hard circular arcs in the entire interval of the subtended angle θ, from the linear segment limit, corresponding to $\theta = 0$, to the circle, corresponding to $\theta = 2\pi$ [Figs. 1(a)–1(e)]. These hard particles are deceptively simple: They are generally concave and, in spite of being infinitesimally thin, they generally exclude an area to one another. The class of circular arcs can be divided into two subclasses: (i) those circular arcs with $\theta \in [0, \pi]$, i.e., minor circular arcs [Fig. 1(f)], from the linear segment limit to the semicircular arc; (ii) those circular arcs with $\theta \in (\pi, 2\pi]$, i.e., major circular arcs [Fig. 1(g)], from the semicircular arc to the circle. Two hard particles of the former subclass can arbitrarily closely approach: e.g., once they are arranged on top of one another. Since this arrangement is replicable ad infinitum, without introducing any overlap, there exist infinitely dense packings of these hard particles. For two hard particles of the latter subclass, this two joint conditions do not hold any more. It is then natural to inquire what are their densest packings and what is the number density that they achieve.

This work attempts to answer this question. Supported by Monte Carlo numerical simulations, one can peculiarly interlace a specific number, depending on θ, of hard major circular arcs to analytically construct compact closed circular groups; one can then arrange these compact closed circular groups on a triangular lattice.

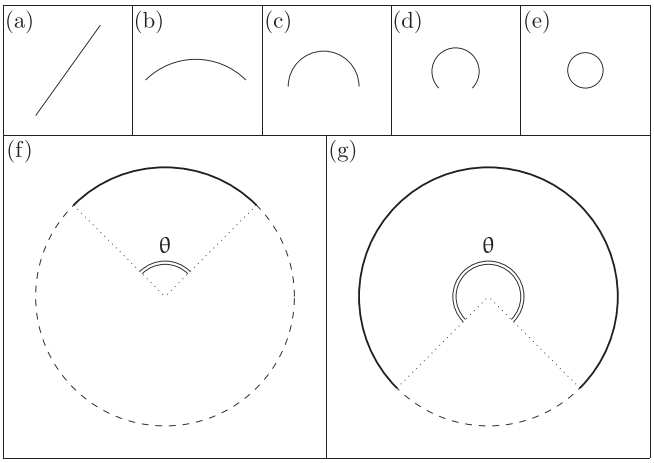

FIG. 1. Examples of circular arcs with different subtended angle θ and equal length: (a) $\theta = 0$; (b) $\theta = \pi/2$; (c) $\theta = \pi$; (d) $\theta = 3\pi/2$; (e) $\theta = 2\pi$. Examples of a minor circular arc with $\theta \leqslant \pi$ (f) and of a major circular arc with $\theta > \pi$ (g): These circular arcs are drawn with a continuous line while the circumferences of their parent circles are drawn with a discontinuous line; the subtended angle θ is explicitly indicated.

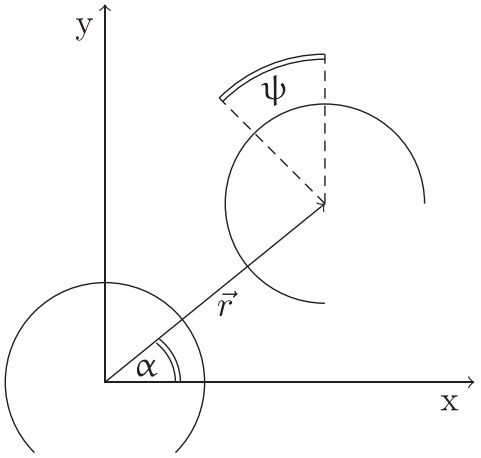

FIG. 2. Two circular arcs in $\mathbb{R}^2$ with the geometric elements that define their pair configuration in a (x,y) Cartesian reference frame: ψ, the angle that the two symmetry axes form; $\vec{r}$, the vector whose modulus is $r = |\vec{r}|$ that joins the centers of the two parent circles; α, the angle that this vector forms with the x axis of the Cartesian reference frame.

To appreciate the mechanism for constructing these compact closed circular groups, it is useful to examine the characteristics of the excluded area of two hard (major) circular arcs (Sec. II A). Once this has been accomplished, the mechanism for constructing compact closed circular groups of a specific number of them is devised; it immediately leads to the densest-known packings by arranging these compact closed circular groups on a triangular lattice (Sec. II B). To asses whether these compact closed circular groups can spontaneously either make up or undo, specific Monte Carlo calculations are then carried out. In general, the closed circular groups that do form on compression in these Monte Carlo calculations have a number of constituent hard major circular arcs smaller than that achievable by analytic construction; the analytically constructed compact closed circular groups are nevertheless able to unfasten on decompression in these Monte Carlo calculations (Sec. III). This suggests that the spontaneous replication of the complete mechanism responsible for the formation of these optimal packings of hard major circular arcs, although possible in theory, will be extremely improbable in practice, but similar suboptimal packings of hard (colloidal, granular) major circular arcs will nevertheless be readily accessible (Sec. IV).

II. EXCLUDED AREA AND CONSTRUCTION OF THE DENSEST-KNOWN PACKINGS

A. Excluded area

In a two-dimensional space, the excluded area of two hard particles is that surface whose constituent points the centroid of one particle cannot occupy due to the presence of the other particle; otherwise, the two hard particles would overlap. For two hard circular particles, the excluded area is the area of a circle whose center coincides with the center of one particle and whose radius is the sum of the radii of the two particles. For two hard noncircular particles, the excluded area depends on their fixed relative orientation. One of them, particle 1, can be held fixed, e.g., with its centroid at the origin of the Cartesian reference frame and an axis along one of the two Cartesian axes, while the other, particle 2, whose axis is rotated by a certain angle ψ with respect to the particle 1 axis, displaces around, freely except for the constraint that it cannot overlap particle 1. While displacing, the particle 2 centroid is as if it effectively generate a region delimited by a boundary; all internal points are prohibited positions for the particle 2 centroid, since, if it occupied one of them, particle 2 would overlap particle 1, while all external points are permitted positions for the particle 2 centroid, since, if it occupies one of them, particle 2 does not overlap particle 1.

Their concavity and infinitesimal thinness make the area that two hard circular arcs exclude to one another peculiar: It deserves an examination.

Since a circular arc is axis-symmetric, it suffices to consider the angle $\psi \in [0, \pi]$. Once ψ has been fixed, a pair configuration of hard circular arcs can be completely defined by $\vec{r}$, the distance vector separating the centers of the parent circles, whose radius is R, with $r = |\vec{r}|$ the modulus of this vector, and α the angle that it forms with the x axis of the Cartesian reference frame (Fig. 2). One can define a function $\mathsf{f}(\vec{r}\,;\psi)$ that takes on the value 1 if the two hard circular arcs overlap and the value -1 if they do not, the overlap condition being established according to an exact and suitable overlap criterion. The excluded-area boundary points can be considered as the zeros of $\mathsf{f}(\vec{r}\,;\psi)$.

Without much loss of generality, one can focus on two hard major circular arcs. In this case, it is very useful to introduce the angle

$$\delta = (\theta - \pi) \in (0, \pi]\,.$$

For each value of δ, one should distinguish between the case $0 \leqslant \psi \leqslant \delta$ and the case $\delta < \psi \leqslant \pi$.

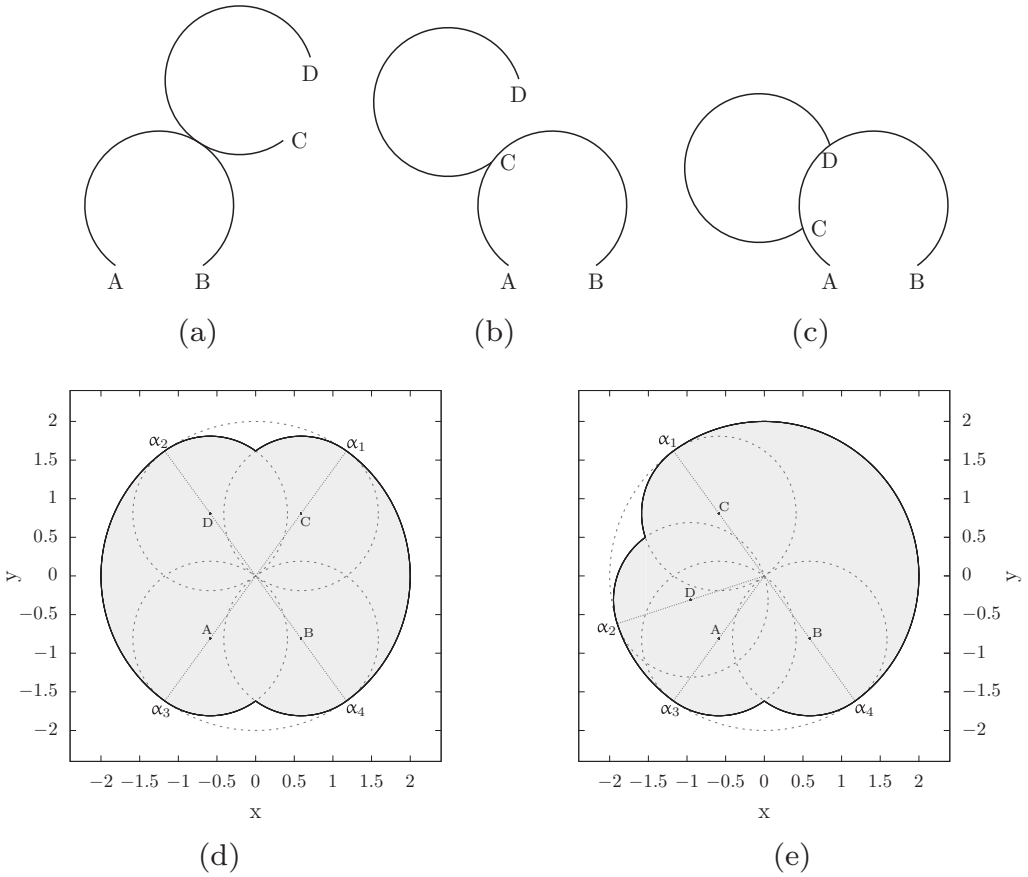

FIG. 3. Examples of three types of contact configuration between two hard circular arcs: (a) internal point – internal point; (b) internal point – extremal point; (c) each extremal point of one hard circular arc respectively touches an internal point of the other hard circular arc. In any of these panels, the extremal points of the hard circular arc held fixed are labeled as A and B while those of the displacing hard circular arc as C and D. The excluded area, the shaded region enclosed by the black continuous line, of two hard major circular arcs with $\theta = 1.6\pi$, i.e., $\delta = 0.6\pi$, for the angle of relative orientation $\psi = 0$ (d) and $\psi = 0.4\pi$ (e). Discontinuous round lines either correspond to the circumference with center (0, 0) and radius $2R$ or to circumferences with the centers that are labeled as the extremal points in panels (a), (b), and (c) and radius R. The special angles are: $\alpha_1 = \frac{\delta}{2} + \psi$; $\alpha_2 = \pi - \frac{\delta}{2} + \psi$; $\alpha_3 = \pi + \frac{\delta}{2}$; $\alpha_4 = 2\pi - \frac{\delta}{2}$. Lengths in panels (d) and (e) are in units of R.

In the case $0 \leqslant \psi \leqslant \delta$, one can distinguish between two situations: Either the two respective contact points at which the two hard circular arcs touch are both internal [Fig. 3(a)] or at least one of these contact points is extremal [Figs. 3(b) and 3(c)]. In the former situation, the two hard major circular arcs behave as two hard circles, with the boundary points that follow a circumference of radius $2R$ [Fig. 3(a)]. In the latter situation, the two hard major circular arcs behave distinctively, with the boundary points that follow a circumference of radius R [Figs. 3(b) and 3(c)]. This latter situation occurs for $\alpha \in (\alpha_1, \alpha_2)$ and $\alpha \in (\alpha_3, \alpha_4)$ with $\alpha_1 = \frac{\delta}{2} + \psi$, $\alpha_2 = \pi - \frac{\delta}{2} + \psi$, $\alpha_3 = \pi + \frac{\delta}{2}$, and $\alpha_4 = 2\pi - \frac{\delta}{2}$ [Figs. 3(d) and 3(e)]. For values of α equal to the midvalues $\alpha_{12} = \frac{\alpha_1+\alpha_2}{2}$ and $\alpha_{34} = \frac{\alpha_3+\alpha_4}{2}$, the two hard major circular arcs touch as peculiarly as in Fig. 3(c): Each extremal point of one of them respectively touches an internal point of the other. On increasing the angle ψ, both extremes of the interval (α_1, α_2) increase of the same quantity ψ with respect to the values that they have at $\psi = 0$ [cf. Fig. 3(d) with Fig. 3(e)]. While the shape of the boundary changes, the area that it encloses does not: The value of the excluded area stays constant throughout the interval $0 \leqslant \psi \leqslant \delta$ [cf. Figs. 3(d) with 3(e): The difference between the area of a circle of radius $2R$ and the excluded area consists of the sum of the two arched triangular regions comprised between α_1 and α_2 and between α_3 and α_4: On going from Fig. 3(d), corresponding to $\psi = 0$, to Fig. 3(e), corresponding to $\psi = 0.4\pi$, the former of these two arched triangular regions rotates round an axis passing through the point $(0, 0)$ and perpendicular to the plane of an angle equal to 0.4π, while the latter of these two arched triangular regions does not change: Hence, that difference does not vary and consequently neither does the excluded area]. It is pertinent to observe that, for $0 \leqslant \psi \leqslant \delta$, the excluded area of two hard major circular arcs coincides with that that two hard lunate particles, formed by the juxtaposition of the same major circular arc with the minor circular arc that subtends the explementary angle (Fig. 4), exclude to one another: For $0 \leqslant \psi \leqslant \delta$, the infinitesimal thinness of two hard major circular arcs and the ensuing capability of them of intertwining do not manifest yet.

In the case $\delta < \psi \leqslant \pi$, the characteristics of the excluded area significantly change. In this case, three rather than two curve sectors in the excluded-area boundary are recognized due to the notable insinuation of two no-overlap

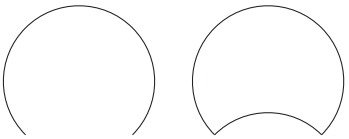

FIG. 4. Comparison between a major circular arc that subtends an angle θ (left) and a lunate particle formed by the juxtaposition of this major circular arc with the minor circular arc that subtends the explementary angle $2\pi - \theta$ (right). Provided that the angle of their relative orientation is $0 \leqslant \psi \leqslant \delta = (\theta - \pi)$, there is no difference between the excluded area of two hard major circular arcs and that of two hard lunate particles.

zones (Fig. 5). The black external curve sector in Figs. 5(d) and 5(e) corresponds to pair contact configurations of hard major circular arcs as arranged as in those pair contact configurations that have been mentioned in the case $0 \leqslant \psi \leqslant \delta$ [Figs. 3(a) and 3(b)]. The dark-gray intermediate curve sector in Figs. 5(d) and 5(e) corresponds to pair contact configurations for which contact occurs on the concave side of one of the two hard major circular arcs [Fig. 5(a)]. The light-gray internal curve sector in Figs. 5(d) and 5(e) corresponds to pair contact configurations for which contact occurs on the convex side of one of the two hard major circular arcs [Fig. 5(b)]. Notably, the two horn-shaped regions delimited by the dark-gray and light-gray curves correspond to nonoverlapping pair configurations. Differently than in the case $0 \leqslant \psi \leqslant \delta$, the two gray curves converge up to the point $(0, 0)$: Provided $\delta < \psi \leqslant \pi$, the point $(0, 0)$ notably belongs to the excluded-area boundary [Figs. 5(d) and 5(e)]. The neighborhoods of the point $(0, 0)$ within the two horn–shaped regions delimited by the dark-gray and light-gray curves, particularly those portions comprised between the two segments tangential to these gray curves, with the angle between these segments indicated as $\Delta\psi$ [Figs. 5(d) and 5(e)], correspond to nonoverlapping pair configurations in which two hard major circular arcs are specially intertwined [Figs. 5(b) and 5(c)]. By a succession

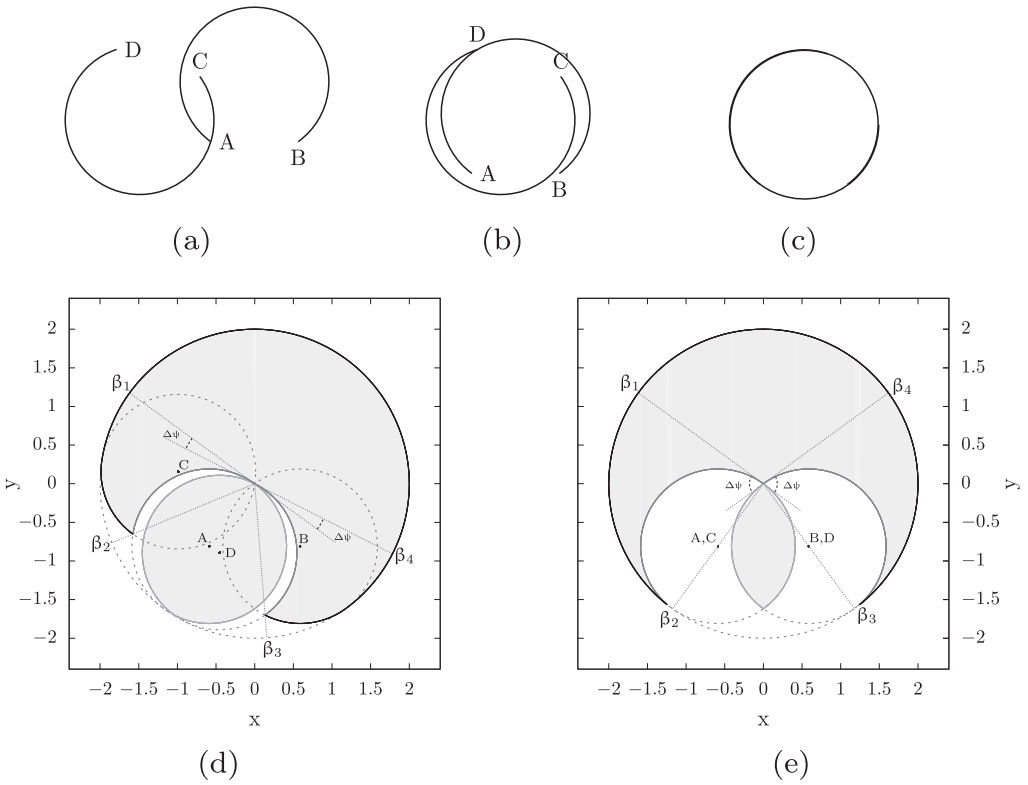

FIG. 5. Examples of three types of contact configuration between two hard major circular arcs in the case $\delta < \psi \leqslant \pi$: (a) the contact involves the concave side of one of the hard major circular arcs: Such contact pair configurations correspond to the dark-gray sector in panels (d), (e); (b) the two hard major circular arcs are intertwined: Such contact pair configurations correspond to the light-gray sector in panels (d), (e); (c) the two hard major circular arcs are so closely intertwined that the centers of their parent circles essentially coincide: Such contact pair configurations correspond to the close neighborhood of the point $(0, 0)$ in panels (d), (e). In any of these panels, the extremal points of the hard major circular arc held fixed have been labeled as A and B while those of the displacing hard major circular arc as C and D. The excluded area, the shaded region enclosed by the union of the black line, the dark-gray line and the light-gray line, of two hard circular arcs with $\theta = 1.6\pi$, i.e., $\delta = 0.6\pi$, for the angle of relative orientation $\psi = 0.65\pi$ (d) and $\psi = \pi$ (e). Discontinuous round lines either correspond to the circumference with center $(0, 0)$ and radius $2R$ or to circumferences with centers that are labeled as the extremal points in panels (a), (b) and radius R. The special angles are: $\beta_1 = \frac{\pi}{2} + \frac{\delta}{2}$, $\beta_2 = \frac{\pi}{2} + \frac{\delta}{2} + \frac{\psi}{2}$, $\beta_3 = \frac{3\pi}{2} - \frac{\delta}{2} + \frac{\psi}{2}$, and $\beta_4 = \frac{3\pi}{2} - \frac{\delta}{2} + \psi$. The angles indicated as $\Delta\psi$ are those formed by the segments starting off at the point $(0, 0)$ and tangential to the dark-gray and light-gray lines; those segments that are tangential to the dark-gray lines correspond to the special angles β_1 and β_4; the amplitude of these angles is $\psi - \delta$. Lengths in panels (d) and (e) are in units of R.

of translatory and, possibly, also rotatory movements, that maintain a value of α within (β_1, β_2) or within (β_3, β_4), with $\beta_1 = \frac{\pi}{2} + \frac{\delta}{2}$, $\beta_2 = \frac{\pi}{2} + \frac{\delta}{2} + \frac{\psi}{2}$, $\beta_3 = \frac{3\pi}{2} - \frac{\delta}{2} + \frac{\psi}{2}$, and $\beta_4 = \frac{3\pi}{2} - \frac{\delta}{2} + \psi$, two hard major circular arcs can come, without overlapping, so close that the centers of their parent circles effectively coincide [Fig. 5(c)]. The amplitude of these angular intervals $\Delta\beta_{12} = \beta_2 - \beta_1$ and $\Delta\beta_{34} = \beta_4 - \beta_3$ is proportional to the angle of relative orientation between the two hard major circular arcs: $\Delta\beta_{12} = \Delta\beta_{34} = \frac{\psi}{2}$. Particularly, by maintaining a value of α within the angular intervals indicated as $\Delta\psi$ [Figs. 5(d) and 5(e)], once the two hard major circular arcs have come so close that the centers of their parent circles effectively coincide, they can then stray around with the guarantee that no overlap occurs between them. The amplitude of $\Delta\psi$ is equal to $\psi - \delta$. Equally as that of $\Delta\beta_{12}$ and $\Delta\beta_{34}$, it linearly increases as the angle of relative orientation between the two hard major circular arcs increases. Thus, on increasing the angle ψ, the two horn-shaped regions and, particularly, the portions associated to $\Delta\psi$ widen [cf. Figs. 5(d) with 5(e)] so that specially intertwined pair configurations such as those in Figs. 5(b) and 5(c) become increasingly more accessible.

That the point $(0, 0)$ belongs to the excluded–area boundary can also occur for hard minor circular arcs. For them, however, the point $(0, 0)$ belongs to this boundary if the value of ψ is sufficiently small down to $\psi = 0$: i.e., two hard minor circular arcs, as they are arranged on top of one another, can arbitrarily closely approach.

This, seemingly minute, difference between the two subclasses of hard circular arcs drastically affects the structure of their dense packings and the corresponding number density. While for hard minor circular arcs there exist infinitely dense packings, this is impossible for hard major circular arcs: Yet, very, albeit finitely, dense packings of them can be analytically constructed exploiting their capability of intertwining, without overlapping, so closely that the centers of their parent circles essentially coincide.

B. Construction of the densest-known packings

That it is possible to closely intertwine two hard major circular arcs (Sec. II A) is exploited to demonstrate that it is actually possible to closely intertwine more hard major circular arcs thus arriving at constructing compact closed circular groups of them. Specifically, it is demonstrated that, for a given angle $\delta = \theta - \pi$, one can arrange $\mathsf{n} = [\frac{2\pi}{\delta}]$, with $[x]$ the strict floor function [20], hard major circular arcs so that the centers of their parent circles essentially coincide without making these hard particles overlap; i.e., n hard major circular arcs essentially arrange on the same circumference, thus maximally exploiting their concavity and infinitesimal thinness.

First, one observes that is impossible to arrange more than n hard major circular arcs on the same circumference. If that were possible, then there would exist a pair of hard major circular arcs whose angle of relative orientation ψ would be smaller than δ. However, as shown in Sec. II A, two such hard major circular arcs would be incapable of approaching so closely to allow the centers of their parent circles to essentially coincide; i.e., they would be incapable of arranging on the same circumference.

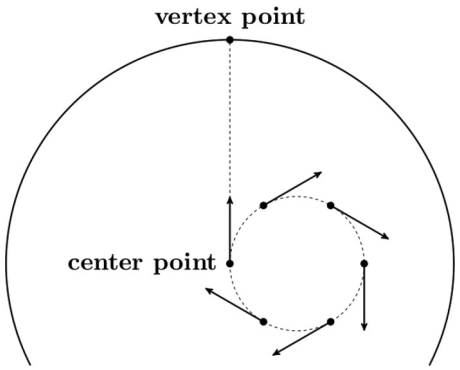

FIG. 6. For hard major circular arcs with $\theta = 1.3\pi$, i.e., $\delta = 0.3\pi$, $\mathsf{n} = 6$. These hard major circular arcs are arranged with the centers of their parent circles on the vertices of a regular convex hexagon and their symmetry axes tangential to the circumscribing circumference whose radius is R_{crf} and (counter) clockwise rotating.

Then, one demonstrates that it is exactly n the number of hard major circular arcs that can be arranged so that the centers of their parent circles essentially coincide; i.e., that can be arranged on the same circumference.

One begins by arranging the centers of the parent circles of these n hard major circular arcs at the vertices of the corresponding regular convex polygon whose characteristic (external) angle is $\delta^* = \frac{2\pi}{\mathsf{n}}$. Consider the circumference that circumscribes this polygon. The n hard major circular arcs are then arranged so that their symmetry axes are tangential to this circumference and (counter) clockwise rotating (Fig. 6 with the example of $\theta = 1.3\pi$, i.e., $\delta = 0.3\pi$, for which $\mathsf{n} = 6$). Provided the radius of this circumference, R_{crf}, is such that $\frac{R_{\mathrm{crf}}}{R} < \frac{\sin(\frac{\delta^* - \delta}{2})}{\sin(\frac{\delta^*}{2})}$, one now demonstrates that no two hard major circular arcs thus arranged can overlap.

By exploiting the regularity of the convex polygon and the symmetry of the system, it suffices to ascertain the absence of an overlap between one hard major circular arc, taken as reference, with any one of the other $\mathsf{n} - 1$ hard major circular arcs. For a given reference hard major circular arc, the angle of relative orientation of the kth other hard major circular arc is $\psi_k = k\delta^*$. Since two relative orientations with angles ψ_k and $\psi_{\mathsf{n}-k} = 2\pi - k\delta^*$ are equivalent, it suffices to consider the angles of relative orientation $\psi_k \leqslant \pi$. It is now useful to refer to the exemplificative and explicative Fig. 7 where, in panel (a), the centers of the six parent circles of the hard major circular arcs are positioned at the vertices of a regular convex hexagon while, in panel (b), the corresponding excluded area of two such hard major circular arcs, whose relative orientation is ψ_k, is depicted for $k = 2$. If the reference hard major circular arc has its symmetry axis aligned along the y axis of the Cartesian reference frame, then one can appreciate that the angle α of the distance vector that joins the center of its parent circle with the center of the parent circle of the kth other hard major circular arc lies midway the special angular interval comprised between the segments that start off at the point $(0, 0)$ and are tangential to the dark-gray and light-gray curves [Figs. 5(d) and 5(e) as well as Fig. 7(b)]. One recalls that the amplitude of this angular interval is $\Delta\psi = \psi_k - \delta$ (Sec. II A). If the angle α is within such an angular interval, then the kth

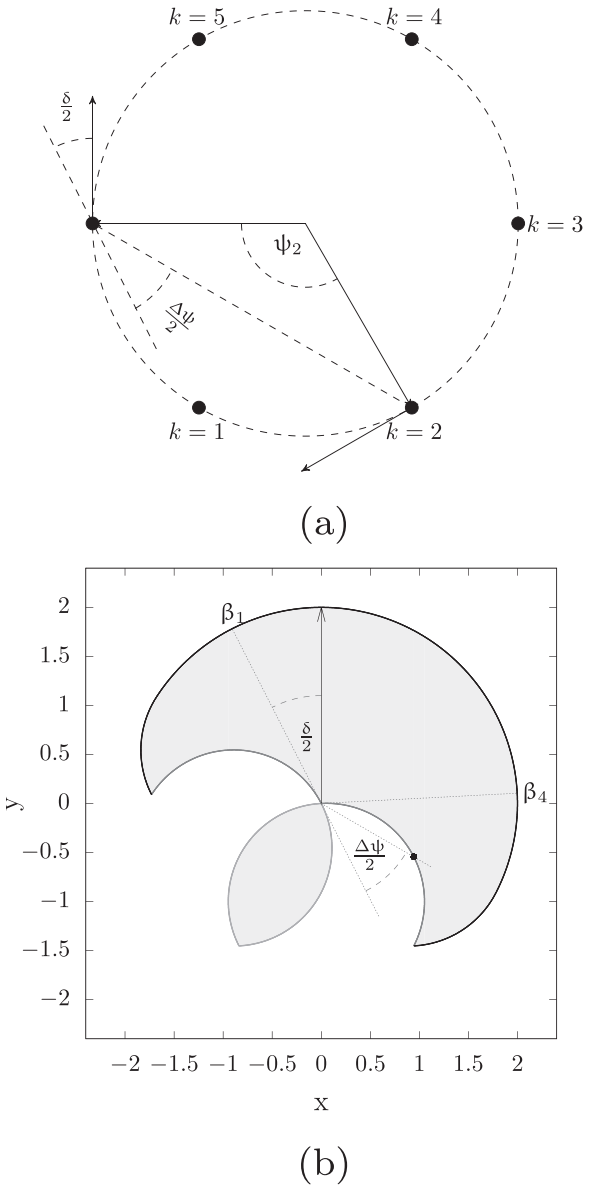

FIG. 7. (a) For a hard major circular arc with a subtended angle θ such that $\mathsf{n} = 6$, the centers of the parent circles are arranged at the vertices of a regular convex hexagon. Consider one hard major circular arc as a reference with its symmetry axis aligned along the y axis of the Cartesian reference frame and the other $k = 1, \ldots, 5$ hard major circular arcs. Out of these, focus on $k = 2$, the hard major circular arc whose symmetry axis forms an angle ψ_2 with the symmetry axis of the reference hard major circular arc. (b) The corresponding excluded area between the reference hard major circular arc and the $k = 2$ hard major circular arc in panel (a). The black filled circle marks the intersection of the segment, that starts off at the point $(0, 0)$ and lies midway between the segments tangential to the dark-gray curve and light-gray curve, with this dark-gray curve. The angles $\frac{\delta}{2}$ and $\frac{\Delta\psi}{2}$ in panel (b) replicate those in panel (a). Lengths in panel (b) are in units of R.

other hard major circular arc can arbitrarily closely approach the reference hard major circular arc. The modulus of the distance that separates the centers of the parent circle of these two hard major circular arcs is equal to $2R_{\mathrm{crf}} \sin(\frac{\psi_k}{2})$. This modulus has to be compared with the modulus of the distance between these two hard major circular arcs that corresponds to the intersection of the mid straight line with the dark-gray curve [black filled circle in Fig. 7(b)]. One can appreciate that this modulus is equal to $2R \sin(\frac{\psi_k - \delta}{2})$. Provided R_{crf} is such that $\frac{R_{\mathrm{crf}}}{R} < \frac{\sin(\frac{k\delta^* - \delta}{2})}{\sin(\frac{k\delta^*}{2})}$, the kth other hard major circular arc does not overlap with the reference hard major circular arc. One can observe that $\frac{R_{\mathrm{crf}}}{R}$ is an increasing function of $k\delta^*$. Thus, it suffices that that condition is verified for $k = 1$. The condition $\frac{R_{\mathrm{crf}}}{R} < \frac{\sin(\frac{\delta^* - \delta}{2})}{\sin(\frac{\delta^*}{2})}$ allows one to progressively shrink the circumscribing circumference on which the centers of the parent circles are positioned without this leading to the n hard major circular arcs overlapping. Thus, as $R_{\mathrm{crf}} \to 0$, the centers of the parent circles ultimately end up to essentially coincide, i.e., the n hard major circular arcs ultimately end up to essentially arrange on the same circumference (Fig. 8).

Having succeeded to construct compact closed circular groups of n hard major circular arcs, it is then natural to arrange these circular groups on a triangular lattice [Fig. 9(a)]. These generally nonlattice and nonperiodic infinitely degenerate [21] packings have a dimensionless number density

$$\rho R^2(\theta) = \frac{1}{2\sqrt{3}} \left\lfloor \frac{2\pi}{\theta - \pi} \right\rfloor = \frac{\mathsf{n}}{2\sqrt{3}}.$$

Observe that the strictness of the floor function that defines n is necessary to recover the densest packing of hard circles and its number density [9] [Fig. 9(c)]. These generally nonlattice and nonperiodic infinitely degenerate packings [21] constitute the densest-known packings for hard major circular arcs.

One different packing strategy could have been to arrange the hard major circular arcs in one of the (non)lattice infinitely degenerate packings where these hard particles are placed on top of one another as in Fig. 9(b) [22]. One can appreciate that the dimensionless number density of all these (non)lattice packings [22] is given by

$$\rho R^2(\theta) = \frac{1}{2\cos\left(\pi - \frac{\theta}{2}\right)\sqrt{4 - \cos^2\left(\frac{\theta}{2}\right)}}.$$

However, it is smaller than that of the packings formed by triangularly arranging the compact closed circular groups of n hard major circular arcs [Fig. 9(c)].

One could have attempted to combine the two packing strategies. First, one essentially arranges a number m of hard major circular arcs on the same circumference by successively rotating them of an angle infinitesimally larger than δ. The number $m = 1, \ldots, \mathsf{p}$, with $\mathsf{p} = [\frac{\pi}{\delta}]$ [20], is sufficiently small that the group thus constructed is generally arched and open with an effective subtended angle equal to $\theta^* = \theta + (m - 1)\delta = \pi + m\delta$. Then, one arranges these arched open groups as it has been done with a single hard major circular arc in Fig. 9(b). The dimensionless number density of such packings is

$$\rho R^2(\theta) = \frac{m}{2\cos\left(\pi - \frac{\theta^*}{2}\right)\sqrt{4 - \cos^2\left(\frac{\theta^*}{2}\right)}}.$$

Irrespective of the value of δ, this function monotonically increases with m, attaining its maximum at $m = \mathsf{p}$, i.e., once

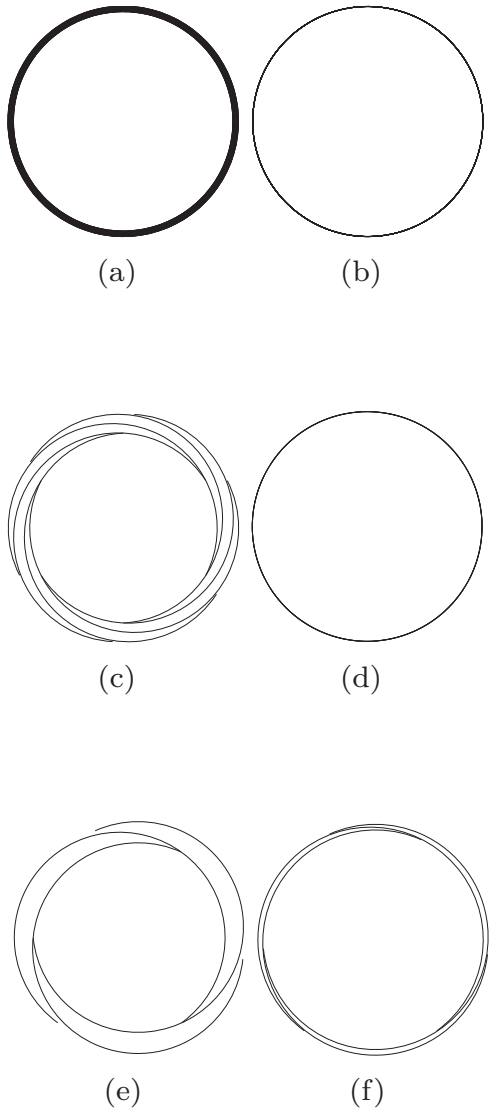

FIG. 8. Examples of the compact closed circular groups that can be analytically constructed: (a), (b) $\theta = 1.05\pi$, i.e., $\delta = 0.05\pi$, leading to $\mathsf{n} = 39$, and (a) $R_{\rm crf} = 0.025$ and (b) $R_{\rm crf} = 2 \times 10^{-12}$; (c), (d) $\theta = 1.3\pi$, i.e., $\delta = 0.3\pi$, leading to $\mathsf{n} = 6$, and (c) $R_{\rm crf} = 0.1$ and (d) $R_{\rm crf} = 4 \times 10^{-5}$; (e), (f) $\theta = 1.6\pi$, i.e., $\delta = 0.6\pi$, leading to $\mathsf{n} = 3$ and (e) $R_{\rm crf} = 0.11$ and (f) $R_{\rm crf} = 0.03$. Lengths are in units of R.

the arched and open groups have actually become closed and circular and ended up to arranging on a triangular lattice. However, $\mathsf{p} < \mathsf{n}$: The circular and closed groups thus constructed are not as numerous as those constructed by the method based on positioning the centers of their parent circles at the vertices of a regular convex polygon: Consequently, the dimensionless number density achieved by these packings is smaller than that of the packings formed by triangularly arranging the compact closed circular groups of n hard major circular arcs.

III. MONTE CARLO CALCULATIONS

One may inquire whether closed circular groups similar to those described in Sec. II B that constitute the structural

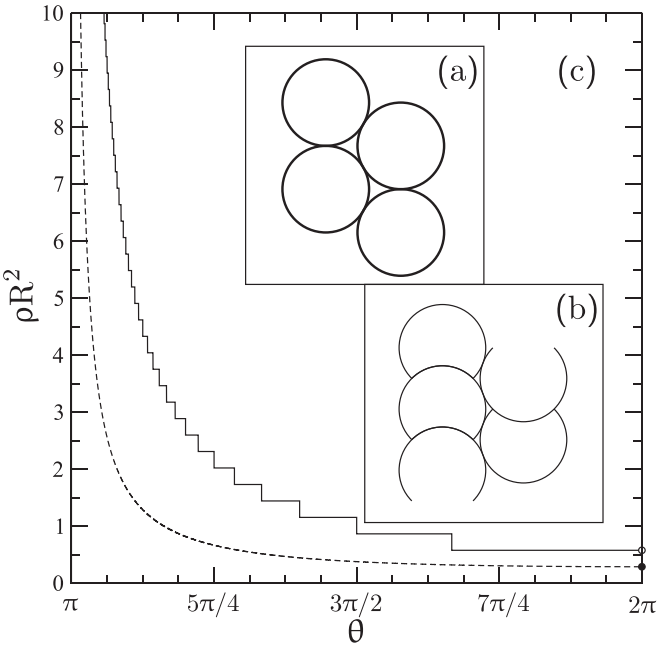

FIG. 9. (a) Portion of a triangular lattice actually formed by the compact closed circular groups of n hard major circular arcs as the thickness of the drawn circumferences wishes to indicate. (b) Portion of a nonlattice formed by hard major circular arcs. (c) Dimensionless number density, ρR^2, as a function of the subtended angle, θ, for the generally nonlattice and nonperiodic compact-closed-circular-group triangular packings (black continuous steplike line) and the (non) lattice packings (black discontinuous monotonic line) of hard major circular arcs. Observe that, for $\theta = 2\pi$, ρR^2 is equal to $\frac{1}{2\sqrt{3}}$ (black filled circle) rather than $\frac{1}{\sqrt{3}}$ (black empty circle) also for the former type of packings, in keeping with the known dimensionless number density of the densest packing of hard circles [9].

units of the densest-known packings of hard major circular arcs may spontaneously form and how compact and numerous they result to be.

To address this point, specific Monte Carlo (MC) [12,14,16] calculations were carried out. In these calculations, systems of N hard major circular arcs in a deformable parallelogrammatic container with hard walls were compressed from a low to a high pressure. The initial value of N was 2. These two hard major circular arcs were initially placed in a large square container with hard walls. The initial value for the dimensionless pressure $P^* = \frac{P\sigma^2}{k_B T}$, with P the pressure, σ^2 the area of that part of a spherical surface subtended by the angle θ, k_B the Boltzmann constant and T the absolute temperature, was 1. Successively, P^* was gradually increased in logarithmic steps up to a value equal to 100. For each of these successive values of P^*, 1 million of MC cycles were usually carried out, with a MC cycle defined as a set of N random translations of a randomly selected particle, N random rotations of a randomly selected particle and one random change of the length and/or orientation of a randomly selected side of the container. In the course of these MC calculations, the maximal sizes for a random translation, a random rotation and a random change of a side of the container were progressively adjusted to ensure that a fraction comprised between 0.2 and 0.3 of each of these trial moves

TABLE I. Largest value of the number of hard major circular arcs per closed circular group, N_i, attained in the ith sequence of Monte Carlo calculations on compression, as well as the corresponding n, as a function of the subtended angle θ.

θ	N_1	N_2	N_3	N_4	N_5	N_6	N_7	n
π	16	17	17	17	17	16	16	∞
1.05π	13	11	11	11	11	12	12	39
1.1π	8	8	9	9	9	9	9	19
1.15π	8	7	8	7	7	7	7	13
1.2π	6	6	6	6	7	6	6	9
1.25π	6	5	5	5	6	5	5	7
1.3π	5	5	5	4	4	5	5	6
$121/90\pi$	4	4	4	4	4	4	4	5
1.4π	4	4	4	4	4	4	4	4
1.45π	3	3	4	3	3	3	3	4
1.5π	3	3	3	3	2	3	3	3
1.55π	2	2	3	2	2	2	2	3
1.6π	2	2	2	2	2	2	2	3
1.95π	2	2	2	2	2	2	2	2
$359/180\pi$	2	2	1	2	2	1	1	2

was accepted. The acceptance of a new shape and a new size for the container was subject to the usual Metropolis criterion of a constant-pressure MC calculation [14,16]. On completion of this sequence of MC calculations, it was observed whether a closed circular group was formed. The number of hard major circular arcs N was then increased by one and the same sequence of MC calculations was repeated for that new value of N. This incremental addition of hard major circular arcs and successive MC-method-based compression of the system were carried on until it was observed that the formation of a closed circular group of N hard major circular arcs did not occur. The largest value of N that led to the formation of a closed circular group was then registered. For a number of values of θ, this entire process was repeated a number of times, usually seven, changing the initial configurations of the N hard major circular arcs and the seed of the random number generator `mt19937` [23]. By operating in this way, Table I was constructed. For a number of values of θ, it reports the seven largest values of N that led to the formation of a closed circular group. These numerical results prove that the spontaneous formation of closed circular groups is indeed possible, even for a value of θ as large as $359/180\pi$. Yet, one has to also observe that these moderately fluctuating largest values of N are usually incapable of equaling the larger number n of hard major circular arcs that is possible to closely intertwine by analytic construction (Sec. II B).

Based on these results, one may then inquire whether the compact closed circular groups that are analytically constructed can spontaneously unfasten when a system of them is decompressed in analogous MC calculations. For values of the angle $\theta \geqslant 1.2\pi$, starting from a dimensionless pressure equal to 100 and decreasing it by logarithmic steps until a value of 0.01 was reached, it proved relatively easy to completely unfasten the analytically constructed compact close circular groups. For values of the angle $\theta < 1.2\pi$, this procedure was insufficient: These more compact and numerous analytically constructed closed circular groups survived down to that very small value of P^*. Nevertheless, they ultimately succeeded to unfasten in relatively painful MC calculations that protracted up to 10^3 million of MC cycles once they were suitably modified so that the random change of the container shape and size was accepted only if it led to a larger container area.

IV. CONCLUSION

In this work, densest-known packings of congruent hard infinitesimally thin circular arcs are analytically constructed. The interest is actually in hard infinitesimally thin major circular arcs whose subtended angle $\theta \in (\pi, 2\pi]$. In spite of being infinitesimally thin, there exists no pair configuration of them where they arbitrarily closely approach and which is replicable ad infinitum, without introducing any overlap, as it occurs for hard infinitesimally thin minor circular arcs whose subtended angle $\theta \in [0, \pi]$. Nevertheless, it is shown that hard infinitesimally thin major circular arcs can be carefully arranged in compact closed circular groups formed by $\mathsf{n} = [\frac{2\pi}{\theta-\pi}]$ [20] of them. These compact closed circular groups can then be arranged with the communal centers at the sites of a triangular lattice thus leading to generally nonlattice nonperiodic infinitely degenerate packings with dimensionless number density equal to $\frac{\mathsf{n}}{2\sqrt{3}}$. These densest-known packings are classifiable as purely entropy-driven cluster (porous) crystals. It is notable that very simple particles, such as these hard infinitesimally thin concave particles, devoid of any attractive or complicated interactions between them, can first cluster and then these clusters act as structural units to form a (porous) crystal. Monte Carlo calculations confirm that these clusters, albeit not as numerous as those analytically constructed, can spontaneously form on compression.

On these premises, the investigation of the complete phase diagram of systems of hard infinitesimally thin circular arcs will prove interesting. Once the latter phase diagram has been mapped, one will possibly move on to considering dense packings and phase behavior of hard finitely thin circular arcs. In actuality, one real example of these systems has been recently investigated [24,25]: Hard colloidal C-shaped particles, corresponding to hard finitely thin circular arcs with $\theta = \frac{3}{2}\pi$, have been prepared and their phase behavior first experimentally investigated in a tilted two-dimensional gravitational column [24] and then theoretically rationalised [25]: Dimerisation has been observed. It is presumable that progressive hard (colloidal, granular) particle thickening will increasingly impede reaching a number of intertwined hard (colloidal, granular) major circular arcs as large as in the infinitesimally thin case but it should still prove interesting to generally examine up to which extent.

ACKNOWLEDGMENT

The authors acknowledge the support of the Government of Spain under Grant No. FIS2017-86007-C3-1-P.

[1] G. Grosso and G. Pastori Parravicini, *Solid–State Physics* (Academic Press, San Diego, 2013); R. Zallen, *The Physics of Amorphous Solids* (Wiley VCH, Weinheim, 2004).
[2] N. H. March and M. P. Tosi, *Introduction to Liquid–State Physics* (World Scientific, Singapore, 2002).
[3] M. P. Allen, G. T. Evans, D. Frenkel, and B. M. Mulder, Adv. Chem. Phys. **86**, 1 (1993).
[4] S. Torquato and F. H. Stillinger, Rev. Mod. Phys. **82**, 2633 (2010).
[5] L. Mederos, E. Velasco, and Y. Martínez–Ratón, J. Phys. Cond. Matt. **26**, 463101 (2014).
[6] M. Dijkstra, Adv. Chem. Phys. **156**, 35 (2015).
[7] C. Avendaño and F. A. Escobedo, Curr. Op. Coll. Interface Sci. **30**, 62 (2017).
[8] S. Torquato, J. Chem. Phys. **149**, 020901 (2018).
[9] L. Fejes Tóth, Mathematische Zeitschrift **46**, 83 (1940).
[10] L. Fejes Tóth, Acta Sci. Math. A **12**, 62 (1950).
[11] G. Kuperberg and W. Kuperberg, Discrete Comput. Geom. **5**, 389 (1990).
[12] N. Metropolis, A. W. Rosenbluth, M. N. Rosenbluth, A. N. Teller, and E. Teller, J. Chem. Phys **21**, 1087 (1953).
[13] B. J. Alder and T. E. Wainwright, J. Chem. Phys. **27**, 1208 (1957).
[14] W. W. Wood, J. Chem. Phys. **48**, 415 (1968); **52**, 729 (1970).
[15] M. Parrinello and A. Rahman, Phys. Rev. Lett. **45**, 1196 (1980); J. Appl. Phys. **52**, 7182 (1981).
[16] M. P. Allen and D. J. Tildesley, *Computer Simulation of Liquids* (Clarendon Press, Oxford, 1987); W. Krauth, *Statistical Mechanics: Algorithms and Computations* (Oxford University Press, Oxford, 2006).
[17] Y. Jiao, F. H. Stillinger, and S. Torquato, Phys. Rev. Lett. **100**, 245504 (2008).
[18] S. Torquato and Y. Jiao, Nature (London) **460**, 876 (2009); Phys. Rev. E **80**, 041104 (2009).
[19] S. Atkinson, Y. Jiao, and S. Torquato, Phys. Rev. E **86**, 031302 (2012).
[20] The strict floor function is $\lfloor x \rfloor = -1 - \lceil -x \rceil$, with $\lceil x \rceil$ the ordinary ceiling function.
[21] These packings are generally nonlattice [4, 8] as their fundamental cell generally contains more than one hard particle. They are also generally nonperiodic [4, 8] as the hard major circular arcs that form a compact closed circular group can be arranged either counterclockwise or clockwise and the compact closed circular groups can be rotated of an arbitrary angle with respect to one another. They are infinitely degenerate as these arbitrary rotations do not affect the value of the number density.
[22] Irrespective as to whether the hard major circular arcs orient the unit vectors that join the center of their parent circle with the respective vertex either parallel, i.e., they form a lattice packing, or antiparallel, i.e., they form a nonlattice packing such as the one in Fig. 9(b), the number density is the same. Each of these (non)lattice packings of hard major circular arcs coincides with the corresponding packing of the corresponding hard lunate particles such as in Fig. 4.
[23] M. Matsumoto and T. Nishimura, ACM Trans. Model. Comput. Simul. **8**, 3 (1998).
[24] P. Y. Wang and T. G. Mason, J. Am. Chem. Soc. **137**, 15308 (2015).
[25] W. D. Hodson and T. G. Mason, Phys. Rev. E **94**, 022124 (2016).